SCIENCE CHINA
Technological Sciences

•Article•

https://doi.org/10.1007/s11431-021-1926-6

Harvesting net power and desalinating water by pressure-retarded membrane distillation

ZHAO RunZe[†], LI Ji[†], ZHANG ZiKang, LONG Rui, LIU Wei & LIU ZhiChun[*]

School of Energy and Power Engineering, Huazhong University of Science and Technology, Wuhan 430074, China

Received June 22, 2021; accepted August 27, 2021; published online October 26, 2021

Pressure-retarded membrane distillation (PRMD) can convert low-grade heat to useful work by harvesting the pressure energy of the condensation liquid on the cold side. In this study, a new type of PRMD system for combined freshwater and power production was proposed. For this configuration, the thermal energy of the phase change is transported to the interface mainly by conduction rather than convection, which significantly reduces the pump power loss of the liquid flow. In addition, it also utilizes a multistage structure to regenerate heat with low pump power loss. The experimental results showed that, for a module with a heating area of 1.0 m^2, this system can produce 188 L of freshwater and 27.8 kJ of power each day when operating between 80°C and 40°C. The water and power densities of the PRMD configuration would be affected by saline ions in the feed liquid, air resistance in the evaporation chamber, membrane wetting, and membrane compaction. The experimental and molecular dynamics simulation results indicated that a higher temperature difference or working temperature will significantly improve the desalination and power generation rates because of the increased mass transfer driving force of the vapor gradient. This study proved that it is possible for a PRMD system to simultaneously obtain net power and freshwater using low-grade heat as the only energy input. Nevertheless, the liquid supply, working pressure, and membrane properties should be improved to achieve better performance.

desalination, renewable energy, low-grade heat, thermo-osmosis, membrane distillation

Citation: Zhao R Z, Li J, Zhang Z K, et al. Harvesting net power and desalinating water by pressure-retarded membrane distillation. Sci China Tech Sci, 2021, 64, https://doi.org/10.1007/s11431-021-1926-6

1 Introduction

A large amount of low-grade heat (below 80°C), which is difficult to convert and often wasted, is produced from solar, geothermal, and industrial activities [1–3]. Pressure-retarded membrane distillation (PRMD) is a new thermal energy conversion technology that utilizes the hydraulic pressure energy of the condensation liquid on the permeation side [4,5]. PRMD was developed from membrane distillation and is also called thermo-osmotic energy conversion [6–8]. As shown in Figure 1(a), a PRMD unit consists of a hydrophobic membrane and two liquid pools. If a transmembrane temperature gradient is added, a vapor pressure difference occurs, which is a driven force of mass transfer. As a result, the liquid on the high-temperature side will transfer across the membrane via evaporation, permeation, and condensation. The volume increment of condensation liquid can drive a hydraulic turbine to harvest electricity in the same manner as pressure retarded osmosis [9]. The power yield of a PRMD unit can be calculated using $W = J_w \cdot \Delta P$, where J_w is the volume rate of the condensation liquid, and ΔP is the working pressure or the transmembrane hydraulic pressure difference.

PRMD technology has advantages, including clear, cheap, and good compatibility. Further, an ideal PRMD circle could achieve better efficiency than other low-grade heat conversion methods [10,11]. Straub et al. [4], Yuan et al. [12], and

†Theses authors contributed equally to this work.
*Corresponding author (email: zcliu@hust.edu.cn)

© Science China Press and Springer-Verlag GmbH Germany, part of Springer Nature 2021

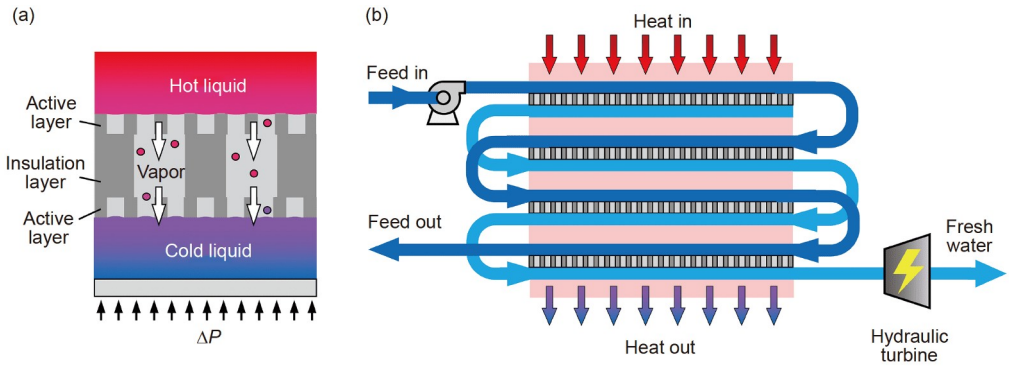

Figure 1 (a) Schematic diagram of PRMD. Two liquid chambers with different temperatures are separated by a hydrophobic nanoporous membrane. During operation, the working liquid will vaporize on the hot side, permeate across the membrane, and then condense to a high-pressure liquid. (b) Schematic illustration of using a multistage PRMD system to obtain pure water and electricity. Driven by a pump, the feed liquid flows across the PRMD stack module. Some water molecules of the feed liquid are transferred across the membranes and converted to high-pressure fresh water. A hydraulic turbine is employed to harvest the pressure energy of the freshwater.

Chen et al. [13] conducted several experiments to investigate the mechanisms of PRMD for harvesting power from low-grade heat sources. Their results showed that the water flux of an actual PRMD module would be affected by the working pressure because of membrane deformation and pore wetting. PRMD technology can also be embedded in a membrane distillation desalination system to recycle electricity. Keulen et al. [14] and Park et al. [15] constructed theory models of two PRMD configurations for combined water and power (CWP) production. Yuan et al. [16] and Mahmoudi et al. [17,18] carried out PRMD experiments for CWP production and found that temperature polarization and concentration polarization in the hydrophilic support layer could significantly reduce the water flux.

Previous PRMD studies have focused on investigating the basic transmembrane mechanism of mass and heat, but their efficiency analyses always did not consider pump power loss. For PRMD systems developed from traditional membrane distillation configurations, the heat for the phase change is transported via liquid convection, causing it to have high liquid flow rates as a result of the large difference between sensible heat and phase change heat. Pump loss can be estimated using the flow rate and pressure drop. Overall, the pump loss increases quickly with the square of the flow rate because pressure drop increases with flow rate. Previous PRMD units have high flow rates in the range of 37.5–210 L/(min m^2) in the hot or the cold channels [12,13,18], leading to a high pump loss relative to the power generation rate. Therefore, an applied PRMD system should reduce the pump power loss to obtain a net power output. In our previous study [19], we developed a stack PRMD system that transports heat mainly by conduction rather than convection. The flow rate of this configuration was very low, less than 0.49 L/(min m^2), and it can function without pump assistance and output net power.

In this study, as shown in Figure 1(b), a new PRMD configuration for CWP that was developed on the basis of the stack PRMD system for power generation only is proposed [19]. For this CWP configuration, the PRMD system transfers heat from the heat source to the interface mainly via conduction rather than convection, enabling the feed flow rate and the pump power consumption to be very low. In addition, to reduce the required heat and improve thermal efficiency, the configuration employs a multistage structure to regenerate heat without increasing excessive pump power loss. To investigate the mechanism of this configuration, a lab-scale system was built, which proved that it is feasible to develop a PRMD system for CWP that can work with low-grade heat as the only energy input. Additionally, a PRMD process with a high-hydraulic-pressure-repellent membrane was simulated using molecular dynamics, which could further the development of PRMD membranes.

2 Materials and methods

A commercial membrane (0.1 μm, Xuanda, China) was used in this study; its properties are listed in Table 1. The membrane has a sandwich structure that can balance the vapor permeability and hydraulic-pressure-repellent ability. Two same active layers made of polytetrafluoroethylene (PTFE) nanofibers exist on the two surfaces of the composite membrane, while the interior is a support layer made of polypropylene microfiber. As shown in Figure 2(a) and (b), the active layer is hydrophobic and has a small nominal pore size of 100 nm, which keeps the membrane from wetting under hydraulic pressure. The support layer reduces the heat conduction loss across the membrane and has a large pore size to reduce the vapor permeating resistance.

As shown in Figure 2(c), the multistage PRMD module with a heating plate has five working stages with six working plates. The working area of each stage is approximately

Table 1 Properties of the membrane employed in the experiment

	Thickness (μm)	Nominal pore size (μm)	Porosity [a)]	Contact angle [b)] (°)
Active layer [c)]	20±6	0.1 [d)]	0.854±0.028	131.3±2.7
Support layer	242±8	20 [e)]	0.605±0.014	142.0±3.4

a) Measured by gravimetric method with isopropyl alcohol as the penetrating media [12]; b) measured by a drop shape analyzer (DSA30, Kruss) via the static sessile drop method; c) the composite membrane has two same active layers attached on two surfaces of the support layer; d) specification from the manufacturer; e) estimated by its scanning electron microscope image.

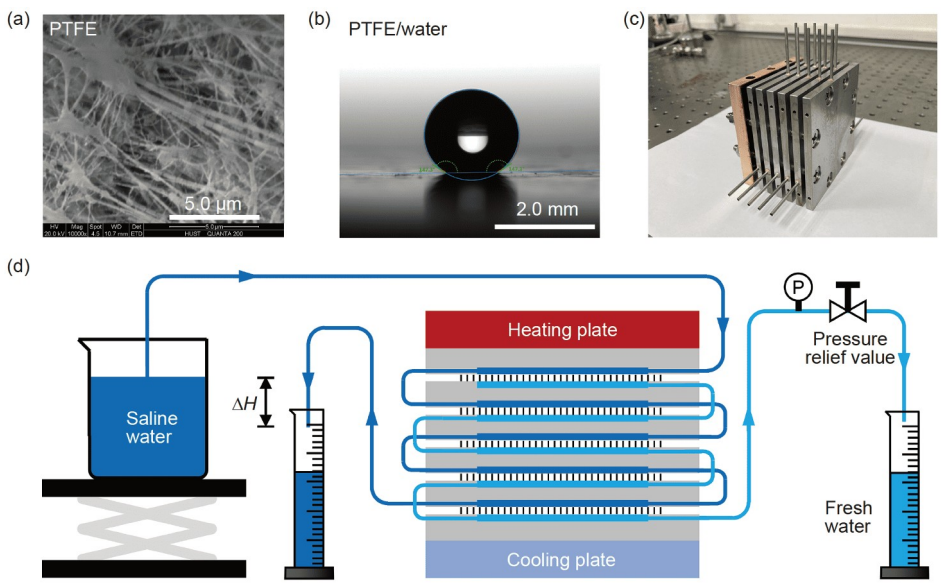

Figure 2 (a) Environmental scanning electron microscope image of the active layer made of polytetrafluoroethylene (PTFE) nanofiber. (b) The active layer of the membrane is hydrophobic to water. (c) Photograph of multistage PRMD module, which was coated with a thermal insulation layer during experimentation. (d) Schematic diagram of the lab-scale PRMD system for energy conversion and desalination.

18 cm^2. Each stage has an evaporation chamber and a condensation chamber on two neighboring plates. The working plates are made of 316 stainless steel to resist the corrosion effect enhanced by saline water. The structure of the working plate is provided in the Appendix. The thicknesses of the evaporation and condensation chambers are approximately 0.1 and 0.3 mm, respectively. The membranes are glued on the working plates and are supported by monel woven meshes. An electrical heating plate and a liquid cooling plate are used as heating sources. When the experiment was conducted, the assembled module was coated by a PTFE insulation layer with a thickness of 20 mm to reduce heat loss to the environment.

The experiment setup is illustrated in Figure 2(d). The feed flow was driven by a hydraulic head. The temperatures of the working plates were obtained by using T-type thermocouples and a data acquisition system (2700, KEITHLEY). The input power of the heating plate was measured using a power meter (PW3335, HIOKI). The temperature of the first working plate was controlled to 50°C, 60°C, 70°C, or 80°C by using a power regulator (TDGC2-2kVA, DELIXI). Meanwhile, the temperature of the last working plate was maintained at 40°C using a liquid temperature control system (WD-1003D, BILON) for all experimental conditions. For the experiment, the cooling system still required pump power to work, while for an application system, the cooling plate can be replaced by a passive cooling device without consuming power. Furthermore, the relatively high temperature of the simulative cooling source can ensure that the real system can achieve the test performance. The outlet rates of feed and freshwater were measured by using graduated cylinders with a suitable range. A needle valve was employed at the fresh water outlet to regulate the working pressure of the PRMD module. The system was leakproof at the tested pressure. Each test condition was carried out for 60 min after equilibrium.

In a real system, the pressure energy of a high-pressure fresh liquid can be converted to electricity via a hydraulic turbine, while the feed flow must consume pump power. The net power rate of the system, W_n, is calculated using

$$W_n = J_{fresh}\Delta P - (J_{feed,out} + J_{fresh})\rho g \Delta H, \quad (1)$$

where J_{fresh} is the yield rate of freshwater, ΔP is the pressure difference, $J_{feed,out}$ is the outlet rate of feed liquid, ρ is the density of feed liquid, g is the gravitational acceleration, and ΔH is the driving hydraulic head of the feed flow. For the

experiment conditions, ΔH was set to 5–90 mm and the $J_{\text{feed,out}}$ was also relatively low, thereby reducing the feed pump loss. In addition, the net power efficiency of the system, η_n, is given by $\eta_n = W_n / Q_{in}$, where Q_{in} is the power input to the electrical heating plate.

The PRMD system visualized by VMD [20] with a high working pressure membrane is shown in Figure 3. The simulation system has a size of 3.97 nm × 3.97 nm × 15.0 nm. It consists of a heating wall, an evaporation chamber with 0.5 mol/L NaCl, a nanofiber PTFE membrane with a pore size of approximately 3.0 nm, a condensation chamber with pure water, and a cooling wall. The force fields of OPLS-AA, TIP3P, and 12-6 LJ/Copper with the geometric combining rule were employed to describe the interactions between atoms [21–23]. The simulations were performed by LAMMPS, with a time step of 1.0 fs [24]. Pressures of 0.1–40.1 MPa were uniformly added to the two wall surfaces. Before the main simulation, the system was pre-equilibrated in NVT assemble for 4.0 ns. For the main process of 40.0 ns, the wall temperature was controlled by the Langevin method, and the rest atoms were simulated in NVE assemble [25–27].

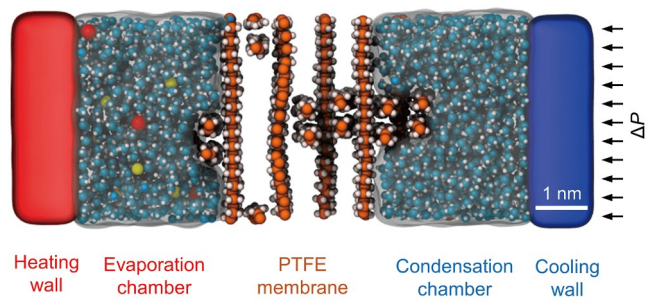

Figure 3 (Color online) Schematic of a molecular dynamic simulation system. It consists of a heating wall, a saline water pool, a nanofiber polytetrafluoroethylene (PTFE) membrane, a freshwater pool, and a cooling wall. The PTFE membrane has a pore size of approximately 3.0 nm and can work at a working pressure of 40 MPa.

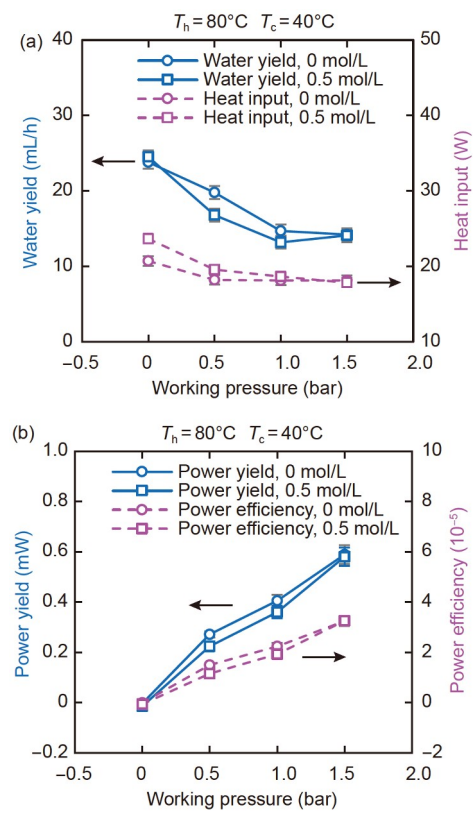

Figure 4 (Color online) Water yield rates, heat inputs (a), and net power generation rates, and net power efficiencies (b) versus the working pressure. The heating and cooling temperatures were fixed at 80°C and 40°C, respectively. The feed liquid was pure water or 0.5 mol/L NaCl solution. The water yield, heat input, power yield, and efficiency are the total values of all stages. Error bar: measuring error.

3 Results and discussion

The PRMD configuration described here has the advantage that the temperature gradient is operated mainly by conduction rather than convection, which can reduce the pump power consumption, thereby generating more net power. Further, the feed rate was less than 0.44 L/(min m^2), which was several orders of magnitude lower than that of traditional PRMD for CWP configurations. In addition, the pump power loss was less than 3.9% of the generated power. Figure 4 shows the performances of the experimental PRMD systems with a feed liquid of saline water or pure water as a function of working pressure. The performances for the pure water feed were slightly better than those with the saline water feed, which is because the saline ions reduce the mass transfer driving force of the vapor pressure gradient. The multistage structure and concentration polarization increased this effect. However, considering the value of freshwater, it is more profitable to use the device for CWP rather than power generation only. Moreover, the device has a high salt rejection rate. For all the tested cases, the NaCl concentration of freshwater production was below 0.005%. For a heating temperature of 80°C and a working pressure of 1.5 bar, it could produce 188 L of high-quality freshwater and generate 27.8 kJ power each day for a 1.0 m^2 heating source area. The generated power can be used for water pretreatment and delivery. Further, the power rate can be improved by employing a high-working-pressure membrane.

As shown in Figure 4(a), the mass and heat transfer rates of the experiment system decreased with decreasing working pressure. The reasons for the relationship include the following: the increment of vapor resistance in the evaporation chamber; the wetting of large pores; and membrane compaction, as shown in Figure 5. During the experiments, the outlet feed liquid was always mixed with a percentage of bubbles that were a mixture of air and vapor. Considering the configuration of the PRMD module, some gas layers should accumulate in the evaporation chamber, thereby increasing

the local vapor transfer resistance [19]. Note that the gas layer would be narrower at a working pressure because of membrane deformation, which increases the vapor transfer resistance. In addition, the active layer may have some large pores, which would become wetted at a working pressure. Pore wetting at the active layer can cause some regions of the support layer to be blocked by wetting, or lead to transmembrane leakage. Furthermore, the membrane is compacted at a working pressure, which may influence the vapor permeability and temperature gradient [12]. For this experiment, membrane compaction should not be the major cause of rate reduction because the support layer has relatively strong mechanical robustness with low porosity [13]. We also found that the rate of decline varied by case. In our previous study [19], three PRMD experiments were performed under the same operating conditions, employing different samples from the same batch. The results showed that two cases did not show a significant water rate decrease under pressure, while one case exhibited a strong declining effect. The difference in pressure responses should not result from membrane mechanic strength because no measurable porosity difference was observed for the test batch. For a multistage PRMD module, it has a large membrane area and is prone to being affected by chamber air resistance and pore wetting. Compared with the PRMD system for power generation only evaluated in our previous study, this system achieved slightly lower power generation because of the larger heat conduction resistance of the working plate, gas in the evaporation chamber, and pore wetting. Therefore, it is important to improve the liquid flow at the evaporation chamber. A possible solution to this problem is improving the liquid supply ability of the capillary structure [28–30]. In addition, it is important to develop high-performance membranes that perform well at high working pressures [31,32].

The performances of the PRMD system for CWP as a function of the heating temperature are shown in Figure 6. For this experiment, the feed liquid was a 0.5 mol/L NaCl solution, and the working pressure was 1.5 bar. The water yield rate increased with the increasing heating temperature because the mass driving force of the vapor pressure difference across the membrane increased with the increasing temperature difference. Note that the water yield rate was near zero when the heating temperature was 50°C. Meanwhile, for the same heating temperature of 50°C and a working pressure of 0 bar, the system can obtain a water yield rate of 2.9 mL/h. However, there should be a transmembrane leakage at a working pressure of 1.5 bar, which reduced the water yield rate from 2.9 to 0.3 mL/h. Thus, for heating sources with a low-temperature difference, it would be better to work only for freshwater rather than CWP.

Figure 7 shows the simulated results of the nanoscale PRMD system as a function of working pressure and heating temperature. The nanoscale system has a very high mass rate

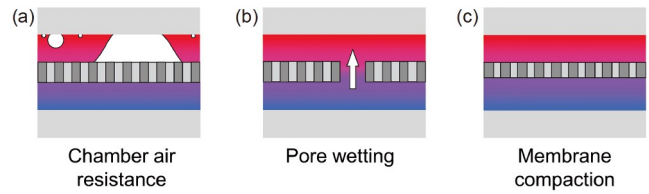

Figure 5 (Color online) Mechanisms of permeation rate loss. (a) Air can accumulate in the evaporation chamber and reduce local flux; (b) some pores with a large size might be wetted at a working pressure and subsequently block vapor transfer or even induce transmembrane leakage from the condensation chamber to the evaporation chamber; (c) membranes are compacted by the working pressure, which affects the permeation rate.

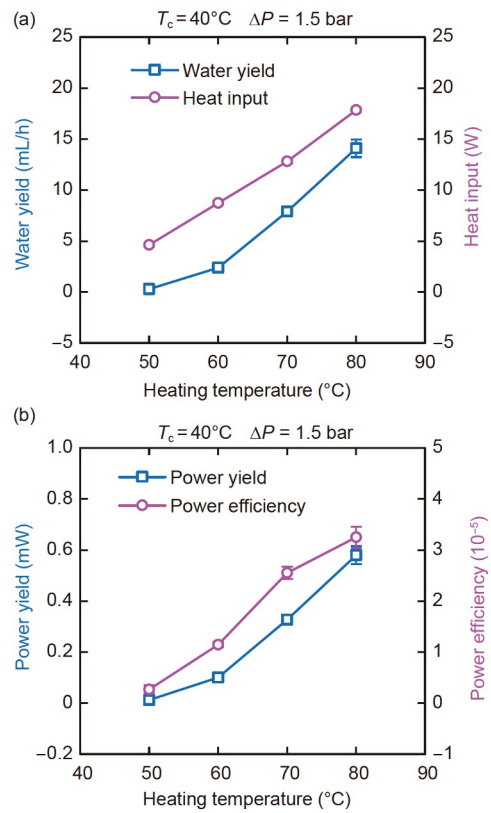

Figure 6 (Color online) (a) Water yield rates and heat inputs of the experiment system versus the heating temperature. (b) Net power generation rates and net power efficiencies versus the heating temperature. The feed liquid was a 0.5 mol/L NaCl solution. The cooling temperature was set to 40°C and working pressure was set to 1.5 bar.

because of its low transfer resistance [33], and the revealed mechanism is helpful because the simulated PTFE membrane can be combined with a thick support layer to a real PRMD system [10]. As shown in Figure 7(a), the nano-fiber membrane with a pore size of approximately 3.0 nm can continue drying at a high working pressure of 40 MPa and would be wetted at a working pressure of 50 MPa. The mass flux was not sensitive to the working pressure because the hydraulic pressure does not significantly influence the transmembrane vapor pressure difference, according to the Kelvin equation [13]. In addition, the pore structure was maintained well. Therefore, it is possible to build a PRMD

system with a high working pressure and power density by developing a high-hydraulic-pressure-repellent membrane with strong robustness [31,34,35]. Further, a high working pressure PRMD system could obtain a very desirable power density and efficiency for a low-grade heat source. Figure 7(b) shows that the water flux of the system increased with heating temperature for the same temperature difference of 40°C. This is because the saturation pressure of the water or saline solution exponentially increases with temperature [36]. Thus, as predicted using the theory calculation [13,19], a PRMD system can perform much better when operating at a higher temperature. The membrane employed in this experiment would not work at a temperature higher than 80°C for a long time because of the tolerance of the support layer. Therefore, it is necessary to develop a PRMD membrane that works at high temperatures. In addition, if the heating temperature is higher than 100°C, the pressure of the feed should be high enough to avoid boiling. Finally, the corrosion resistance of the device must also be considered for CWP production.

4 Conclusions

In this study, a PRMD system that utilizes low-grade heat for CWP production was proposed. For this configuration, to reduce flow loss, the heat for the phase change is mainly transferred via conduction rather than convection. In addition, it has a multistage structure to regenerate heat in order to reduce heat consumption. A lab-scale experiment system with 5 working stages and composite membranes was constructed. The resultant system had a very low pump power loss and could yield fresh water and net power simultaneously. Specifically, for a module with a heating area of 1.0 m^2, it could produce 188 L freshwater and 27.8 kJ power in 24 h when operating between 80°C and 40°C. The results show that saline ions of feed would slightly reduce the water flux and power density of the PRMD system. Further, a higher working pressure produced a better power output rate, but it reduced the desalination rate, which may be the result of increased air resistance, membrane wetting, and membrane compaction. In addition, the experiment and simulation results indicate that a higher temperature difference or working temperature will significantly improve the desalination and power generation rates because of the larger mass transfer driving force. To achieve higher performance of the PRMD configuration, the liquid supply to reduce the extra air resistance in the evaporation chamber should be improved and high-performance membranes that can work at high working pressures, and high temperatures should be developed.

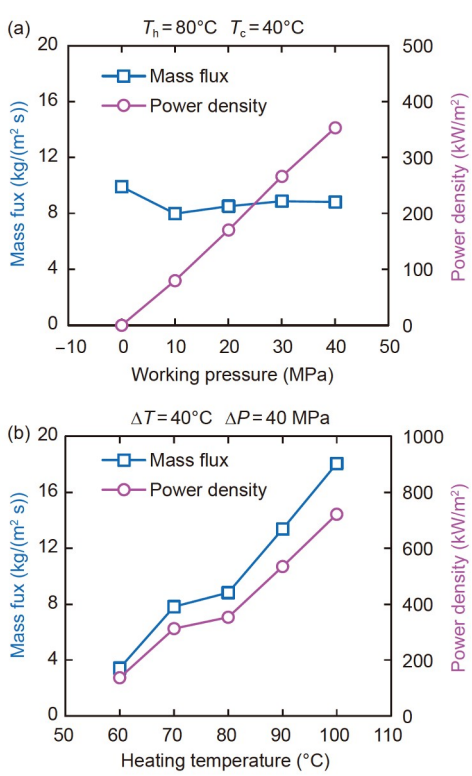

Figure 7 (Color online) (a) Performance of the molecular dynamics simulation system at different working pressures. The heating temperatures were kept at 80°C and 40°C. (b) Performance of the simulation system at different heating temperatures. The temperature difference of the sources was fixed at 40°C and the working pressure was set to 40 MPa.

Appendix

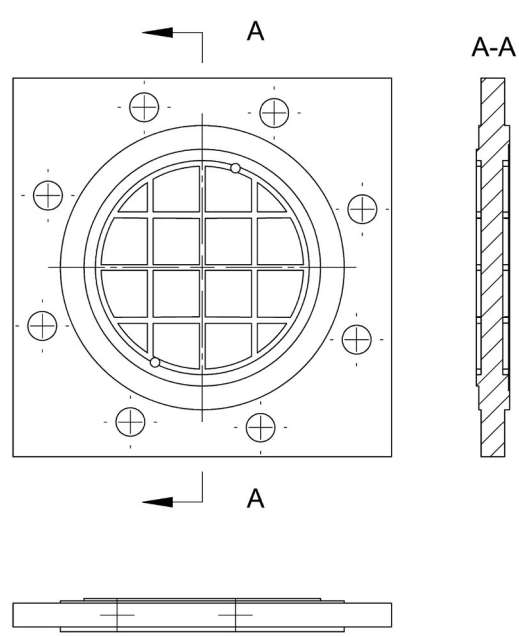

Figure A1 Structure of the working plate.

This work was supported by the National Natural Science Foundation of China (Grant Nos. 51776079 & 52076088), the China Postdoctoral Science Foundation (Grant No. 2020M672344), and the Open Research Fund of Key Laboratory of Space Utilization, Chinese Academy of Sciences (Grant No. LSU-KFJJ-2019-07).

1 Gingerich D B, Mauter M S. Quantity, quality, and availability of waste heat from united states thermal power generation. Environ Sci Technol, 2015, 49: 8297–8306
2 Lu H, Price L, Zhang Q. Capturing the invisible resource: Analysis of waste heat potential in chinese industry. Appl Energy, 2016, 161: 497–511
3 He K, Wang L. Time to change the energy conservation direction of China's steel industry: From upgrading the technology level to increasing scrap ratio. Sci China Tech Sci, 2020, 63: 128–139
4 Straub A P, Yip N Y, Lin S, et al. Harvesting low-grade heat energy using thermo-osmotic vapour transport through nanoporous membranes. Nat Energy, 2016, 1: 16090
5 Kuipers N, Hanemaaijer J H, Brouwer H, et al. Simultaneous production of high-quality water and electrical power from aqueous feedstock's and waste heat by high-pressure membrane distillation. Desalin Water Treat, 2015, 55: 2766–2776
6 Deshmukh A, Boo C, Karanikola V, et al. Membrane distillation at the water-energy nexus: Limits, opportunities, and challenges. Energy Environ Sci, 2018, 11: 1177–1196
7 Bamasag A, Alqahtani T, Sinha S, et al. Experimental investigation of a solar-heated direct contact membrane distillation system using evacuated tube collectors. Desalination, 2020, 487: 114497
8 Barragán V M, Kjelstrup S. Thermo-osmosis in membrane systems: A review. J Non-Equilibrium Thermodyn, 2017, 42: 217–236
9 Bajraktari N, Hélix-Nielsen C, Madsen H T. Pressure retarded osmosis from hypersaline sources — A review. Desalination, 2017, 413: 65–85
10 Straub A P, Elimelech M. Energy efficiency and performance limiting effects in thermo-osmotic energy conversion from low-grade heat. Environ Sci Technol, 2017, 51: 12925–12937
11 Xu Z, Zhang L, Zhao L, et al. Ultrahigh-efficiency desalination via a thermally-localized multistage solar still. Energy Environ Sci, 2020, 13: 830–839
12 Yuan Z, Wei L, Afroze J D, et al. Pressure-retarded membrane distillation for low-grade heat recovery: The critical roles of pressure-induced membrane deformation. J Membrane Sci, 2019, 579: 90–101
13 Chen X, Boo C, Yip N Y. Low-temperature heat utilization with vapor pressure-driven osmosis: Impact of membrane properties on mass and heat transfer. J Membrane Sci, 2019, 588: 117181
14 Keulen L, van der Ham L V, Kuipers N J M, et al. Membrane distillation against a pressure difference. J Membrane Sci, 2017, 524: 151–162
15 Park K, Kim D Y, Yang D R. Theoretical analysis of pressure retarded membrane distillation (PRMD) process for simultaneous production of water and electricity. Ind Eng Chem Res, 2017, 56: 14888–14901
16 Yuan Z, Yu Y, Wei L, et al. Pressure-retarded membrane distillation for simultaneous hypersaline brine desalination and low-grade heat harvesting. J Membrane Sci, 2020, 597: 117765
17 Mahmoudi F, Date A, Akbarzadeh A. Further investigation of simultaneous fresh water production and power generation concept by permeate gap membrane distillation system. J Membrane Sci, 2019, 572: 230–245
18 Mahmoudi F, Date A, Akbarzadeh A. Examining the commercially available hydrophobic membranes in combined desalination and power generation through permeate gap membrane distillation. Desalination, 2020, 474: 114149
19 Li J, Zhang Z, Zhao R, et al. Stack thermo-osmotic system for low-grade thermal energy conversion. ACS Appl Mater Interfaces, 2021, 13: 21371–21378
20 Humphrey W, Dalke A, Schulten K. VMD: Visual molecular dynamics. J Mol Graphics, 1996, 14: 33–38
21 Jorgensen W L, Maxwell D S, Tirado-Rives J. Development and testing of the OPLS all-atom force field on conformational energetics and properties of organic liquids. J Am Chem Soc, 1996, 118: 11225–11236
22 Jorgensen W L, Chandrasekhar J, Madura J D, et al. Comparison of simple potential functions for simulating liquid water. J Chem Phys, 1983, 79: 926–935
23 Heinz H, Vaia R A, Farmer B L, et al. Accurate simulation of surfaces and interfaces of face-centered cubic metals using 12–6 and 9–6 lennard-jones potentials. J Phys Chem C, 2008, 112: 17281–17290
24 Plimpton S. Fast parallel algorithms for short-range molecular dynamics. J Comput Phys, 1995, 117: 1–19
25 Fu L, Merabia S, Joly L. Understanding fast and robust thermo-osmotic flows through carbon nanotube membranes: Thermodynamics meets hydrodynamics. J Phys Chem Lett, 2018, 9: 2086–2092
26 Li J, Long R, Zhang B, et al. Nano heat pump based on reverse thermo-osmosis effect. J Phys Chem Lett, 2020, 11: 9856–9861
27 Li J, Gao S, Long R, et al. Self-pumped evaporation for ultra-fast water desalination and power generation. Nano Energy, 2019, 65: 104059
28 Chen R, Lu M C, Srinivasan V, et al. Nanowires for enhanced boiling heat transfer. Nano Lett, 2009, 9: 548–553
29 Nam Y, Ju Y S. A comparative study of the morphology and wetting characteristics of micro/nanostructured Cu surfaces for phase change heat transfer applications. J Adhes Sci Tech, 2013, 27: 2163–2176
30 Wen R, Li Q, Wang W, et al. Enhanced bubble nucleation and liquid rewetting for highly efficient boiling heat transfer on two-level hierarchical surfaces with patterned copper nanowire arrays. Nano Energy, 2017, 38: 59–65
31 Shaulsky E, Karanikola V, Straub A P, et al. Asymmetric membranes for membrane distillation and thermo-osmotic energy conversion. Desalination, 2019, 452: 141–148
32 Ma T, Yang C, Guo W, et al. Flexible Pt_3Ni–S-deposited Teflon membrane with high surface mechanical properties for efficient solar-driven strong acidic/alkaline water evaporation. ACS Appl Mater Interfaces, 2020, 12: 27140–27149
33 Nazari M, Masoudi A, Jafari P, et al. Ultrahigh evaporative heat fluxes in nanoconfined geometries. Langmuir, 2019, 35: 78–85
34 Jian S, Zhu J, Jiang S, et al. Nanofibers with diameter below one nanometer from electrospinning. RSC Adv, 2018, 8: 4794–4802
35 Hemeda A A, Esteves R J A, McLeskey Jr J T, et al. Molecular dynamic simulations of fibrous distillation membranes. Int Commun Heat Mass Transfer, 2018, 98: 304–309
36 Wang X J, Lafon P, Sundaram D, et al. Liquid vaporization under thermodynamic phase non-equilibrium condition at the gas-liquid interface. Sci China Tech Sci, 2020, 63: 2649–2656